# New developments in multiconfigurational Quantum Chemistry

**Per Åke Malmqvist, Steven Vancoillie, Victor P. Vysotskiy and Valera Veryazov**

*Theoretical Chemistry, Chemical Center, P.O.B. 124, Lund 22100, Sweden*

Multiconfigurational methods in Quantum Chemistry are precise and reliable tools to study the electronic structure of ground and excited states of molecular systems. The recent developments of multiconfigurational methods implemented in the MOLCAS package [1] opens up new horizons for research in the field.

## Parallelization of CASPT2 code

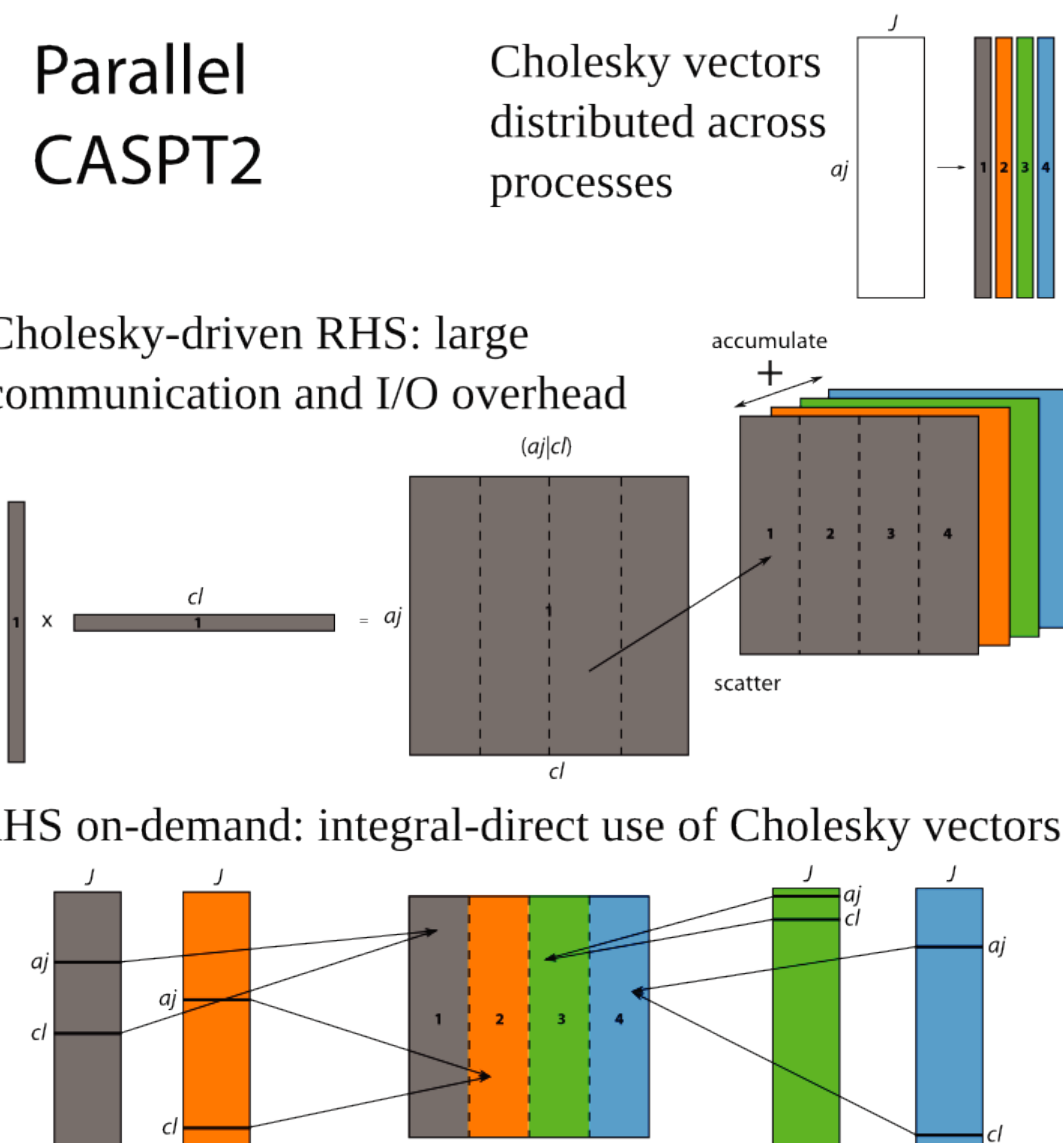Challenges in parallelization of CASPT2 [2]

Active Density Matrices ($\sim N^6_{act}$)
- scales well (independent tasks)
- tasks bound by memory bandwidth
- diagonalization handled by ScaLAPACK

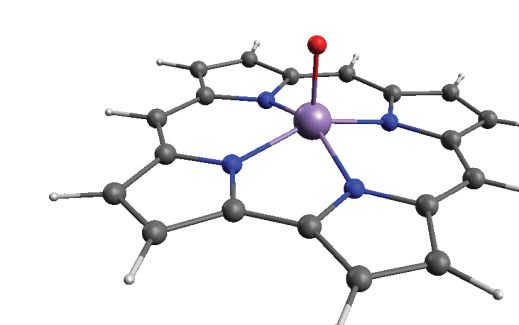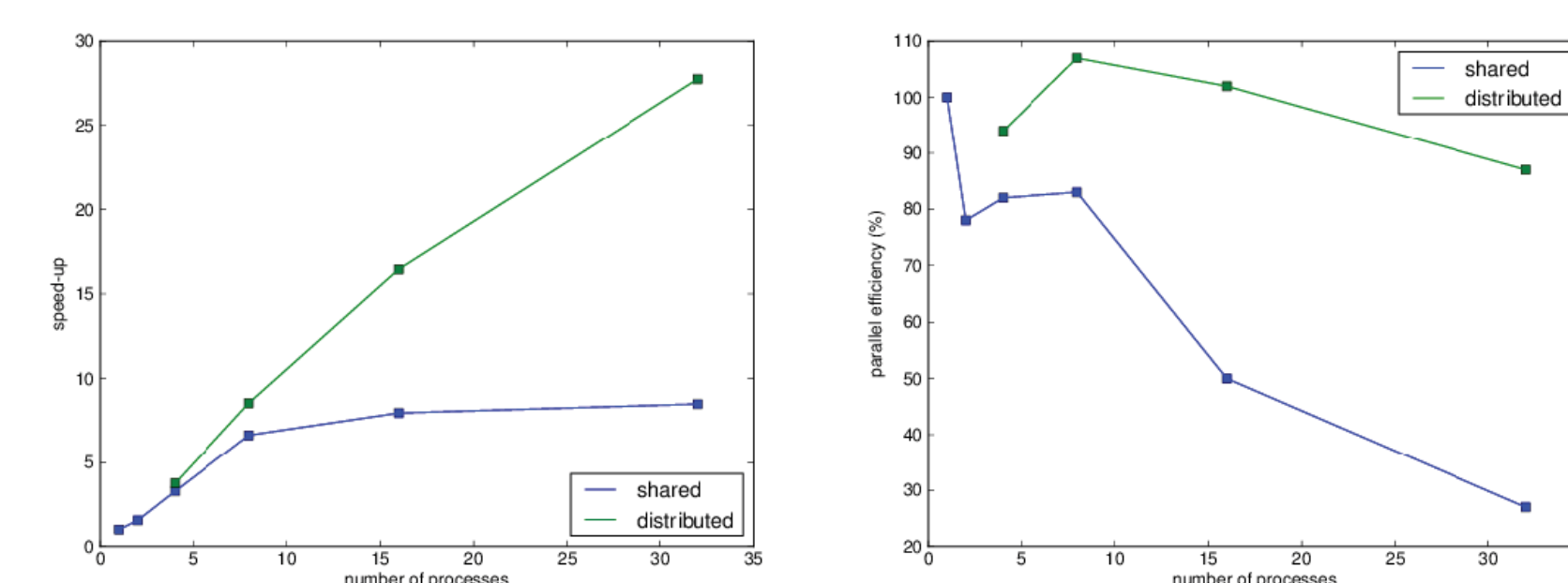Right Hand Side ($\sim N^2_{inact} N^2_{virt}$)
- scales reasonable
- tasks bound by memory bandwidth
- tasks bound by memory/process

Preconditioned Conjugate Gradient
- scales poorly (in theory not scalable)
- lots of communication
- tasks bound by memory bandwidth

Parallel CASPT2



Cholesky vectors distributed across processes

Cholesky-driven RHS: large communication and I/O overhead

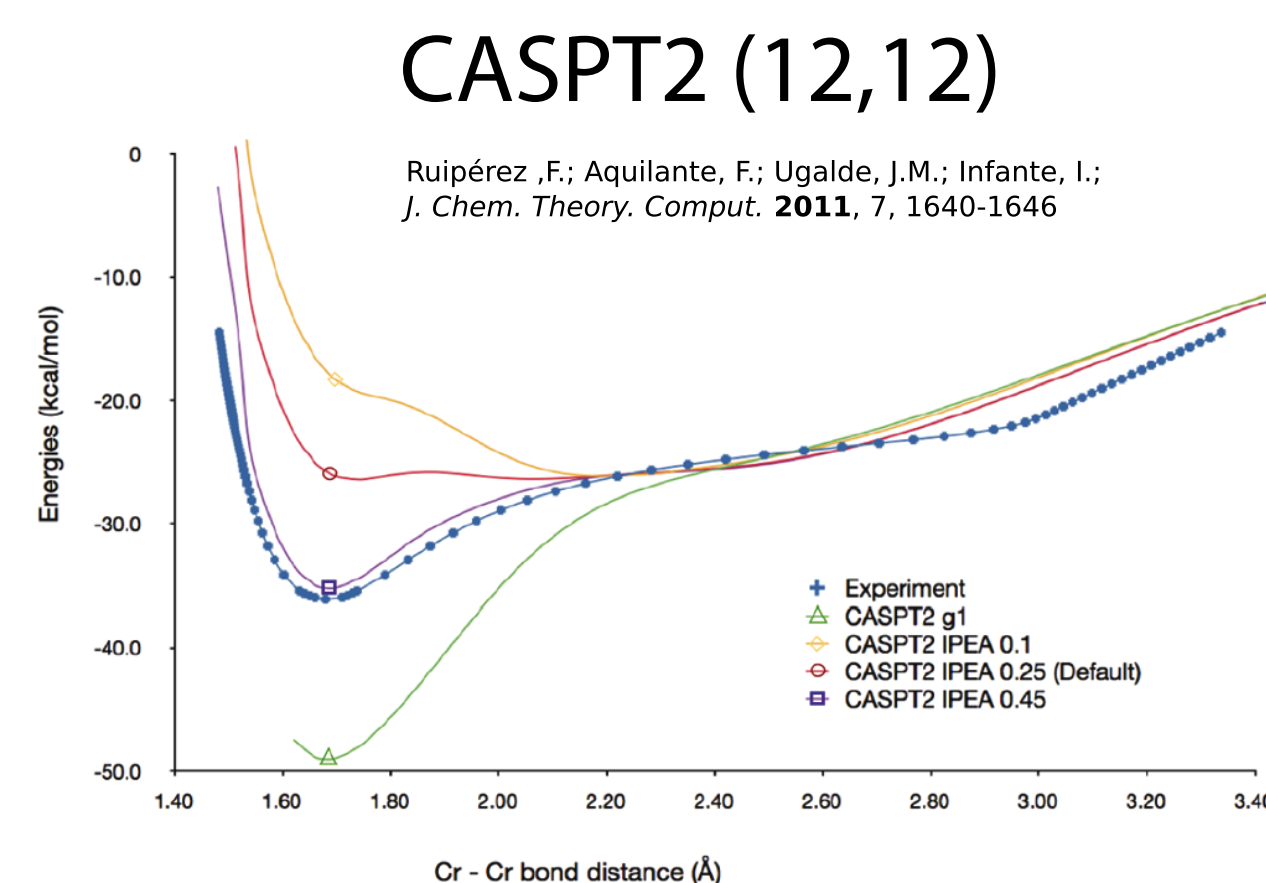RHS on-demand: integral-direct use of Cholesky vectors

### RASPT2 (527 bfn. 35 active orbitals)



Speed-up in 3-body density matrix diagonalization, PCG limits scalability

## RASPT2: state-of-the-art calculations of chromium dimer

The ground state potential curve of the chromium dimer ($Cr_2$) has long been a challenging test case for computational quantum chemistry.

### CASPT2 (12,12)



Ruipérez, F.; Aquilante, F.; Ugalde, J.M.; Infante, I.; *J. Chem. Theory. Comput.* **2011**, 7, 1640-1646

There is a strong dependence on the IPEA shift when using a limited active space that does not include the double-shell effect. The IPEA shift was empirically set to 0.45 a.u. to match the experimental curve

### RASPT2 (12,22)/(12,12)/SD
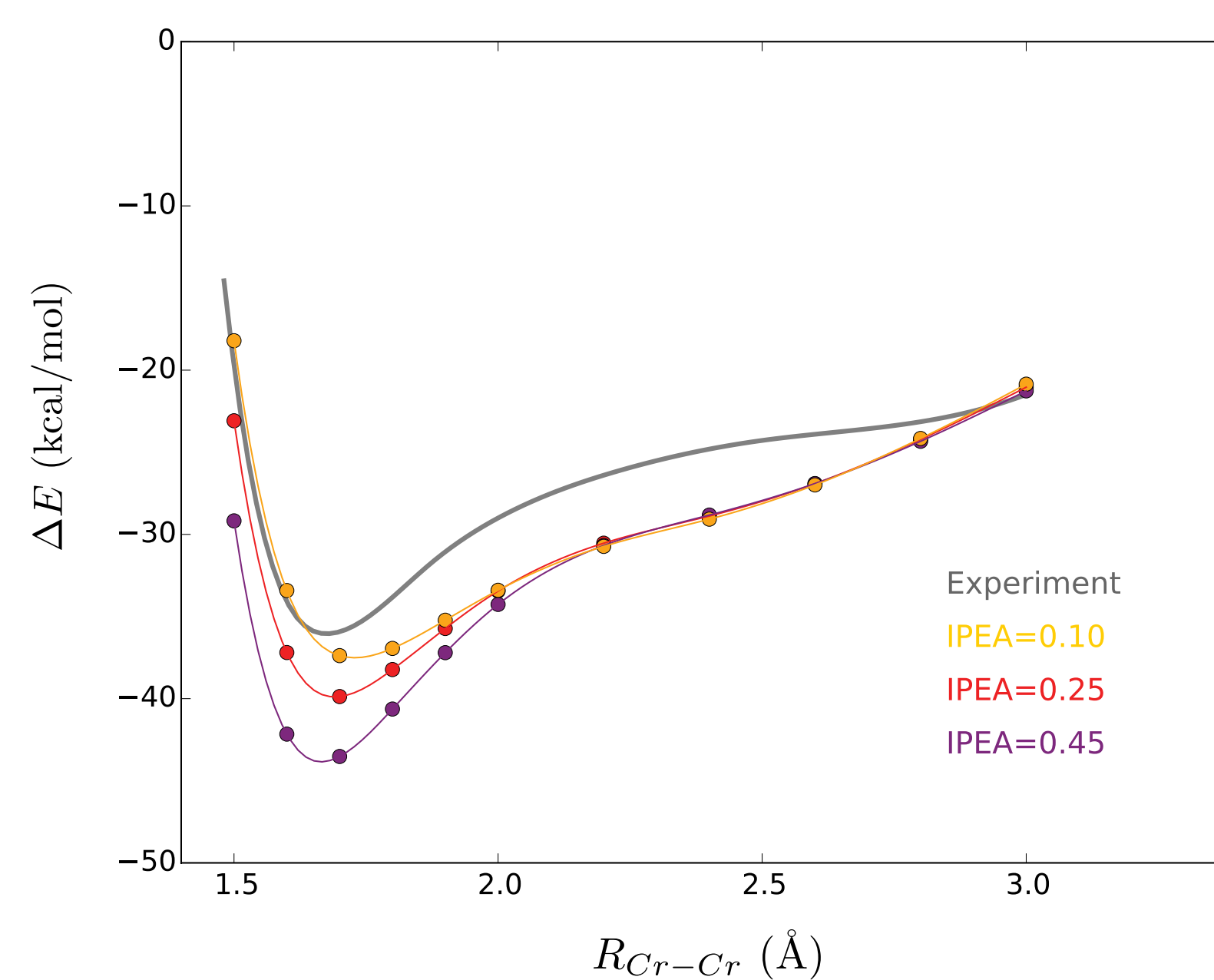


### Computational cost:

| $Cr_2$ $D_{2h}$ 360 bfn | |
| --- | --- |
| Integrals (CD) | 12 min |
| CASSCF(12,12) | 2 min |
| CASPT2(12,12) | 1 min |
| RASSCF(12,22)/(12,12)/SD | 12 h |
| RASPT2(12,22)/(12,12)/SD | 1 h |
| RASSCF(12,22)/(12,12)/SDTQ | 21h (CI only) |
| RASPT2(12,22)/(12,12)/SDTQ | 5h (parallel 4x2) |
| hardware: 2.2GHz Intel Xeon E5-2660 (8 cores) 32Gb RAM | |

When including the full double-shell effect in a RAS3 space with single and double excitations, the IPEA dependency is much smaller, and the default value (0.25 a.u.) is satisfactory. The bonding energy is within 5.0 kcal/mol of the experimental value, and the calculated PES parallels the experimental curve.

## Binatural orbitals for any state functions
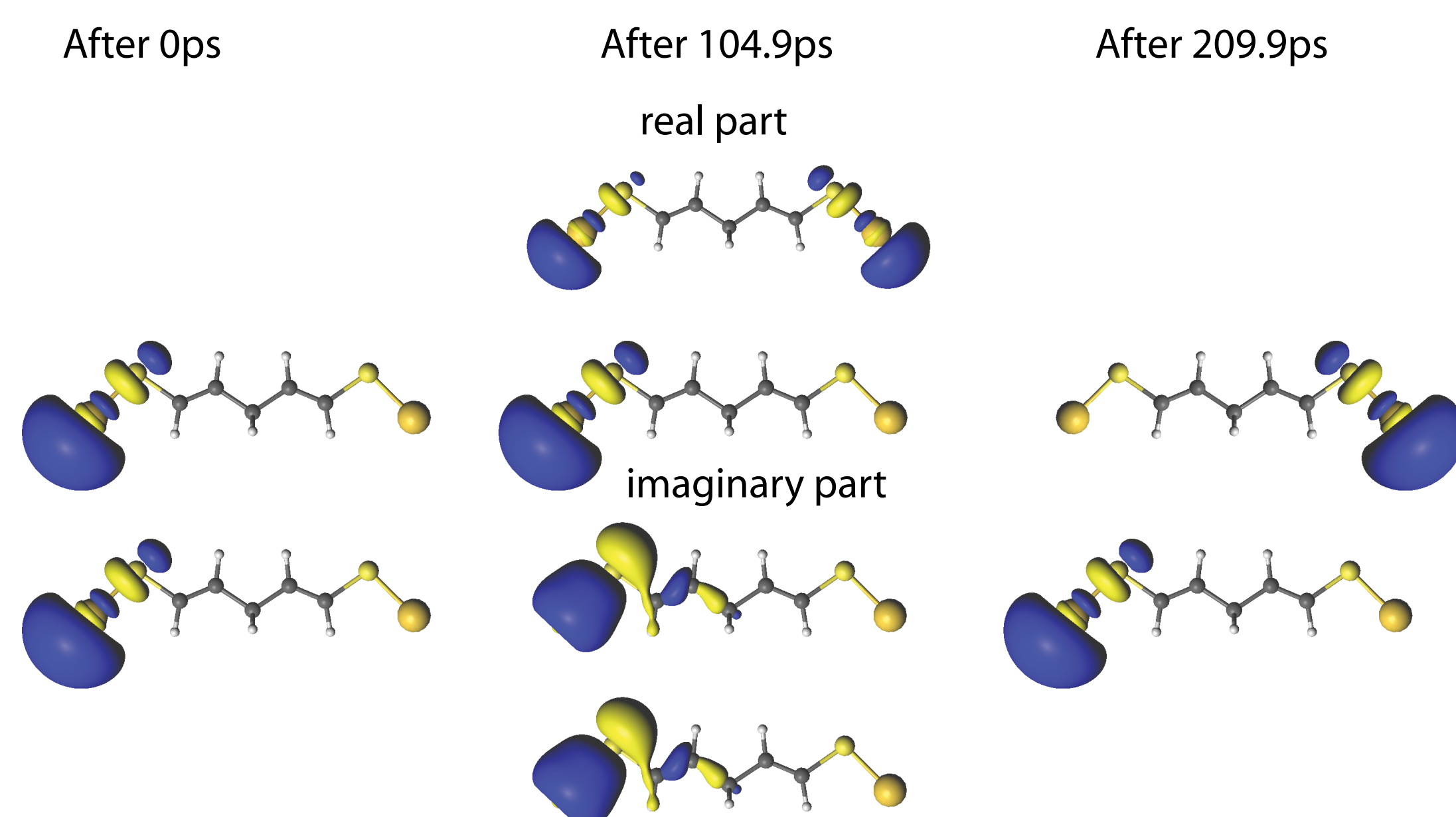
For two state functions $\Psi_1$ and $\Psi_2$, the bra and the ket binatural orbitals [3] express concisely the transition density matrix:

Dominating binatural orbitals of time-dependent electron transfer in Au-PDDT-Au. (Bra orbital above, ket below)



After 0ps     After 104.9ps     After 209.9ps

real part

imaginary part

$$\gamma(\mathbf{r}_1, \mathbf{r}_2) = \sum_K \lambda_K \phi_K^{Bra}(\mathbf{r}_1)\phi_K^{Ket}(\mathbf{r}_2)$$

where the sum over K is short (typically 1-3).

The binatural orbitals represent the propagator,

$$\left\langle \Psi(t)|\hat{\phi}^\dagger(\mathbf{r}_1)\hat{\phi}(\mathbf{r}_2)|\Psi(0)\right\rangle \text{ where } |\Psi(t)\rangle = \exp(-i(\hat{H}-E)t|\Psi(0)\rangle$$

Bra and ket orbitals at times 0ps, 105ps and 210ps. Starting at time 0, the electron is on the left Au atom. After 210ps, it has moved to the right Au atom. At intermediate times, the orbitals are complex; the ket orbital is similar to that of the original transition density, the real part of the bra orbital has a growing amplitude on the right Au and a shrinking one on the left Au. The interplay of real and imaginary part reflects the current density. Current flows, although slowly, and there is never much radical density on the PDDT chain.

## CASPT2 calculations of water dissociation on oxide surfaces

### Dissociation of water molecule on MgO and CaO surface.

Surface model: cluster $M_{14}O_6$ (M=Mg,Ca) embedded into electrostatic field and AIMP pseudo-atoms; partially frozen fragments [4].
Initial geometry scan of water position on the surface: DFT/B3LYP, followed by CASSCF/CASPT2 calculation (12/12)
Physical sorption (no structural changes neither at surface or at adsorbed molecule) of water leads to two geometries: with two hydrogen bonds (PS*) or with one hydrogen bond (PS). Chemical sorption (CS) includes possible dissociation and surface relaxation

MgO: no dissociation of water
CaO if all atoms on the surface are fixed: no dissociation
CaO with surface relaxation: barrier free dissociation



Water dissociation on CaO surface
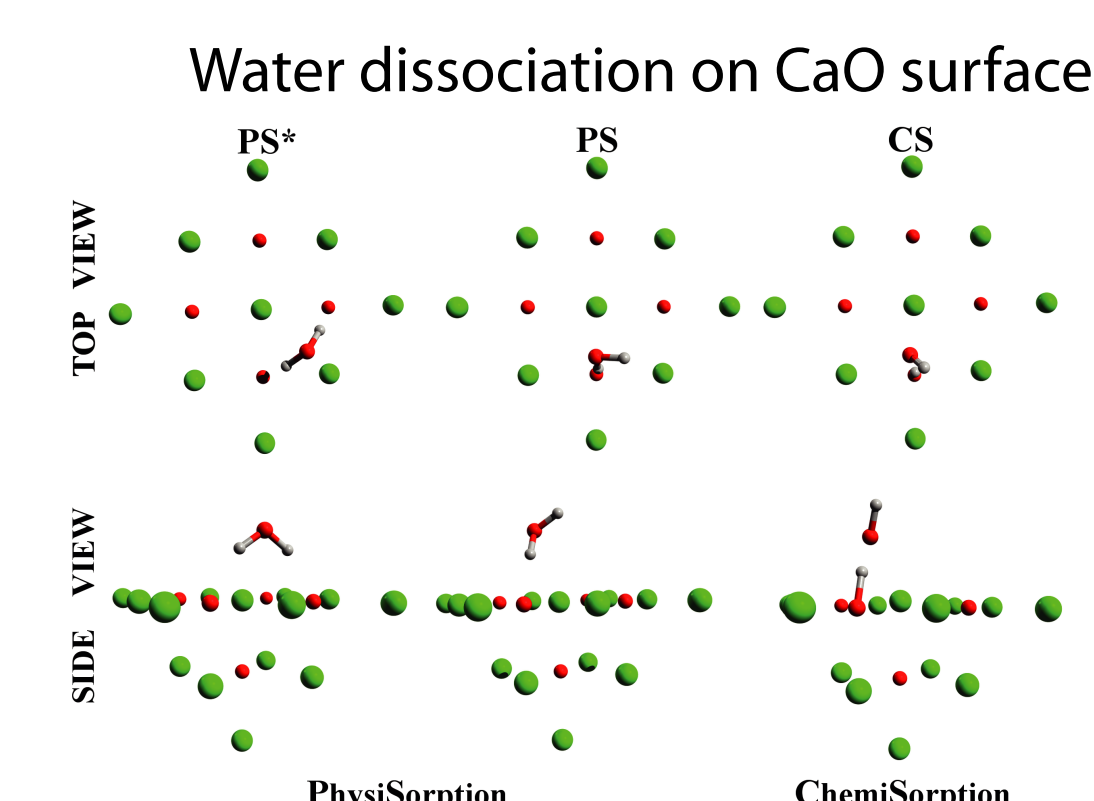
## References:

[1] F. Aquilante, L. D. Vico, N. Ferré, G. Ghigo, P. Å. Malmqvist, P. Neogrády, T. B. Pedersen, M. Pitoňák, M. Reiher, B. O. Roos, L. Serrano-Andrés, M. Urban, V. Veryazov, R. Lindh, "MOLCAS-7: The next generation", J. Comput. Chem. 31, 224–247 (2010).
[2] S. Vancoillie, M. G. Delcey, R. Lindh, V. Vysotskiy, P-Å. Malmqvist, V. Veryazov, "Parallelization of a multiconfigurational perturbation theory", J. Comp. Chem. 34, 1937–1948 (2013)
[3] P. Å. Malmqvist, V.Veryazov, "The binatural orbitals of electronic transitions", Mol. Phys. 110, 2455-2464 (2012)
[4] V. P. Vysotskiy, J. Boström, V. Veryazov "A new module for constrained multi-fragment geometry optimization in internal coordinates implemented in the Molcas package", J. Comp. Chem., 34, 2657-2665 (2013).

http://www.molcas.org